Hydrodynamic interactions and enhanced energy harnessing amongst many WEC units in large-size wave parks

Journal of *Marine Science and Engineering*

MDPI

Article

Hydrodynamic Interactions and Enhanced Energy Harnessing amongst Many WEC Units in Large-Size Wave Parks

Xinyuan Shao [1,*], Jonas W. Ringsberg [1,*], Hua-Dong Yao [1], Uday Rajdeep Sakleshpur Lokesh Gowda [1], Hrishikesh Nitin Khedkar [1] and Jørgen Hals Todalshaug [2]

[1] Department of Mechanics and Maritime Sciences, Division of Marine Technology, Chalmers University of Technology, SE-41296 Gothenburg, Sweden
[2] CorPower Ocean AB, SE-12630 Hägersten, Sweden
* Correspondence: xinyuan.shao@chalmers.se (X.S.); jonas.ringsberg@chalmers.se (J.W.R.)

Abstract: Interactions between wave energy converters (WECs) can significantly affect the overall energy-harnessing performance of a wave park. Although large-size wave parks with many WEC units are commonly considered in practical applications, it is challenging to simulate such parks due to huge computational costs. This paper presents a numerical model that uses the boundary element method (BEM) to simulate wave parks. Each wave energy converter (WEC) was modelled as a comprehensive system, including WEC buoys, power take-off, and mooring systems, with hydrodynamic interactions included. Two classical layouts for arranging 16 units were simulated using this numerical model. The energy-harnessing performance of these array layouts was analyzed for both regular waves and a selection of irregular sea state conditions with different wave directions, wave heights, wave periods and water depths. For each layout, three WEC separation distances were studied. An increase of up to 16% in the power performance of the WEC under regular waves was observed, which highlights the importance of interaction effects.

Keywords: hydrodynamic interaction effects; renewable energy; wave energy; wave park

Citation: Shao, X.; Ringsberg, J.W.; Yao, H.-D.; Gowda, U.R.S.L.; Khedkar, H.N.; Todalshaug, J.H. Hydrodynamic Interactions and Enhanced Energy Harnessing amongst Many WEC Units in Large-Size Wave Parks. *J. Mar. Sci. Eng.* **2024**, *12*, 730. https://doi.org/10.3390/jmse12050730

Academic Editors: Rodrigo Carballo Sánchez, Iván López Moreira, Mario López Gallego, Carlos Pérez-Collazo and Victor Ramos

Received: 8 April 2024
Revised: 22 April 2024
Accepted: 25 April 2024
Published: 27 April 2024

1. Introduction

Wave energy is a promising renewable energy source that has attracted increasing attention in the global market [1,2]. It shows larger power density and round-the-clock characteristics compared with solar and wind energy [3]. However, wave energy converter (WEC) technology has not converged to a certain design like solar panels or wind turbines, which explains the existence of many different kinds of WECs. Falcão [4] classified WECs into oscillating water columns, oscillating bodies and overtopping devices. Different working principles of WECs result in varied requirements for physical tests and numerical modelling. This situation hinders the development of WEC technology.

To harness wave energy cheaply, a typical solution is to install multiple WECs in an area, which constitutes a wave park (also called wave farm or WEC array), to reduce cost by sharing anchors, moorings, power cables, and other subsea installations. The side effect is that, as shown by the pioneering works of Budal and Falnes [5,6], the hydrodynamic interactions caused by diffracted and radiated waves between WECs can be constructive or destructive to the power output depending on the array's layout and sea state conditions, such as the wave height, wave period, wave encounter direction and water depth. In addition to the hydrodynamic interactions, there are also mechanical interactions caused by shared moorings, floaters and mechanically connected WEC components, which also influence the overall power performance of WECs in a wave park [7,8]. Moreover, the influence of the interaction effects goes far beyond changes in the power output. Basin tests in [9] indicate a potential increase in mooring loads when installing multiple WECs in an array.

Various studies have been conducted on wave parks to address the influence of the interaction effect and guide wave park designs, with the number of WECs ranging from two to over one thousand. In the most simple wave park, a 2-WEC array, the interaction effects already play an important role in power performance and mooring fatigue damage. In [10], for medium separation distances ranging from 10 to 50 times the diameter of the WEC, the interaction can be low or high depending on the configuration, especially when the wave direction is not aligned with the array. For larger separation distances, such as 75 times the WEC diameter as described in [7], the hydrodynamic interaction has only a weak influence on the calculated power interaction. However, it results in a significant impact on mooring fatigue damage, ranging from an 80% reduction to a fourfold increase.

As the number of WECs increases, the complexity of the effects also builds up. Stallard et al. [11] analysed a 3-WEC rectilinear array, and the results indicate that if the waves align with the array, the performance of the middle WEC can be improved. Krivtsov and Linfoot [9] tested a 5-WEC array and found that the extreme peak mooring loads in the leading mooring line were approximately doubled in similar environmental conditions compared to those in a single device. Göteman [12] simulated a 6-WEC array with 1000 layouts. The study showed that the difference in power absorption between the best and worst layout is 23%, which indicates that the influence of the hydrodynamic interactions is non-negligible, and the interactions can play a positive role with well-designed layouts. Both [11,13] studied 9-WEC arrays with three rows and three columns. The results in [11] showed that the interactions are constructive along the front row but decay with distance through the array; moreover, the interaction factor is highly dependent on the settings of the power take-off (PTO) system. Lamprou et al. [13] varied the wave direction and found that the central WEC within the array has the largest positive interaction under 0-degree waves. However, no clear rules exist for other wave directions about whether the interaction effects are constructive or destructive among various WECs.

To further investigate the potential of wave parks, many studies went beyond 10-WEC arrays. For a 12-WEC array in [14], the interaction factors appear to vary with both incident wave conditions and device location within the array. The authors also found that there was row attenuation across the array in the direction of wave propagation in short-period waves, consistent with [11]. Integrating multiple WECs with an offshore wind turbine platform has been a hot research topic in recent years [15–20]. Interactions between WECs and wind turbine platforms can be seen as a continuation of the conventional WEC–WEC interaction problem, which also involves hydrodynamic and mechanical interaction. A hybrid system was studied in [15] with 24 WECs and four wind turbines. The multiple array configuration adopted by this wind–wave hybrid platform is beneficial when the wave direction is 0 degrees. However, this finding cannot be generalized to other wave directions, which is the same conclusion as in [13].

There are macroscopic studies of wave parks with more than 50 devices. The employment of such large-scale arrays lowers power fluctuation. As found in [21], doubling the number of WECs from 50 to 100 decreases the power variance by approximately 21%; doubling it from 100 to 200 decreases the power variance by approximately 19%. However, for large farms and realistic irregular sea states, the interaction effects are more likely to be destructive [22].

The ways to study interaction effects can be roughly classified into two groups: experiments and numerical simulations. Stallard et al. [11] conducted experiments with arrays of three, nine and twelve identical WECs. Weller et al. [14] studied a 12-WEC array (4×3) experimentally. Stratigaki et al. [23] presented their experimental study of a 25-WEC array. Similar experimental studies were conducted by Rahm et al. [24], da Fonseca et al. [25], Wolgamot et al. [26], and Ruiz et al. [27]. However, studying interaction effects through experiments has two major drawbacks. Firstly, the results of an experiment usually correspond to a certain set of testing parameters and a specific WEC prototype, so they cannot be generalized to a different set of parameters or a different WEC prototype easily and reliably. This becomes even worse during the wave park design process when parameters

are supposed to evolve continually. Moreover, experiments for large-scale wave parks carried out in wave tanks are usually scaled down, which introduces not-well-understood scaling effects. Secondly, the experiments' economic, time, and human resource costs are high.

Numerical simulations are becoming popular in the preliminary design of WECs and wave parks because of their high-speed and low-cost features. The most commonly used approach is the boundary element method (BEM), which has been adopted to analyse the interaction effects in many studies, such as Sinha et al. [28], Tay and Venugopal [29], Yang et al. [7], and Shao et al. [30]. HydroD, WAMIT, and ANSYS Aqwa are three software programs based on BEM with a wide audience. The BEM method is based on linear potential theory and cannot consider severe sea conditions. Due to the limitation of the total amount of meshes in BEM software, the number of WECs is therefore restricted. Also, the detailed modelling of PTO and mooring systems is still uncommon because of their complexity and software limitations. The most feasible method for large-scale WEC arrays with over 50 devices is analytical multiple scattering theory, which can consider hydrodynamic interactions based on linear potential flow theory. However, all studies using this method have made compromises to reduce the computational cost. Göteman et al. [22] introduced an interaction cut-off distance, which eliminates the interaction effects between WECs when their distance is beyond a threshold. Göteman et al. [21] included interactions by radiated waves but neglected the diffraction between WECs; their model has not been validated or verified for large arrays, so their results only provide quantitative references for future WEC array designs.

From the above literature review, the challenges faced by wave park designers and researchers can be summarized as follows: (1) lack of general rules to guide the design process without limiting the WEC type, dimensions, and wave conditions. (2) lack of reliable and fast numerical tools that consider the complete system, which includes the WEC buoy, the PTO system and the mooring system. (3) Lack of efficient modelling methods to predict large-size parks with many units considering most of the primary hydrodynamic and mechanical interaction effects. (4) Lack of systematic analysis of various factors influencing a wave park's power performance. Specifically, the challenges (2)–(4) will be partly addressed in this study.

In this paper, a BEM-based modelling method is developed to push the computation limit up to 16 WEC units within a park. This number has not been achieved for this type of method until now. Compared to the method proposed by Göteman et al. [21,22], the BEM-based modelling method takes into account all interaction effects. To validate this modelling approach, a general sensitivity based on CorPower Ocean's WEC, which is a representative type of bottom-fixed heaving point absorber, is carried out to investigate the power performance of two kinds of 16-WEC array layouts concerning the distance between WEC units, wave conditions and the shape of the arrays. The WEC model takes complete consideration of the buoy's hydrodynamic characteristics, including the viscous drag force and the end-stop feature of the PTO system. This study contributes to the understanding of how the power performance of wave parks is affected by multiple factors and provides valuable reference data for future wave park design.

The remainder of this paper is structured in the following way. Section 2 gives a general description of the theory behind the used method. Section 3 explains the numerical model emphasising the drag elements, the PTO system and the power performance calculation. Section 4 introduces the two 16-WEC layouts and the studied sea state conditions. Section 5 presents the results of the simulations with discussion. Section 6 summarizes the findings and makes conclusions.

2. Theory

2.1. Linear Potential Theory and the BEM

Linear potential theory assumes the fluid is inviscid and incompressible while the fluid motion is irrotational. Under this assumption, the fluid can be fully described by the

Laplace equation and the Bernoulli equation with prescribed boundary conditions. BEM is a method to solve the velocity potential in the Laplace equation by deploying sources or a mixture of sources, sinks and dipoles over the mean wetted surface. After obtaining the velocity potential, the Bernoulli equation can be applied to obtain the pressure on the wetted surface. The total hydrodynamic forces can be obtained by integrating pressure over the wetted surface. Further details on linear potential theory and BEM can be found in [31,32]. The BEM solver HydroD [33] was employed for simulations in the present study.

2.2. WEC Hydrodynamics and Interaction Effects

The hydrodynamic forces of a WEC unit are computed in the frequency domain. In this paper, the interaction effects refer to the hydrodynamic interactions caused by the radiation and diffraction between different WECs in the flow field. The total velocity potential for a flow field, including multiple interacting bodies, can be expressed under the framework of linear potential theory in the frequency domain as follows:

$$\varphi(\boldsymbol{X})e^{-i\omega t} = \left[(\varphi_I + \varphi_d) + \sum_{m=1}^{M}\sum_{j=1}^{6}\varphi_{rjm}x_{jm}\right]e^{-i\omega t}, \tag{1}$$

where φ_I and φ_d are the velocity potentials of the incident and diffracted waves, φ_{rjm} is the unit radiation potential due to the unit j-th motion of the m-th structure, $\boldsymbol{X}$ is the position coordinates of any point inside the flow field and x_{jm} is the motion amplitude of that structure. The time-varying feature of the potentials is represented by $e^{-i\omega t}$, where t is the time, and ω is the wave frequency. The total potential is solved first, and then the corresponding wave excitation force, added mass and damping for different wave frequencies ω are obtained.

2.3. WEC Dynamics

The WEC system can be represented as a rigid body dynamic system by integrating hydrodynamic forces, hydrostatic forces, mooring and power take-off (PTO) forces into the equation of motions:

$$\boldsymbol{M}\ddot{\boldsymbol{X}} = \boldsymbol{F}_{hydrodynamic} + \boldsymbol{F}_{hydrostatic} + \boldsymbol{F}_{mooring} + \boldsymbol{F}_{PTO} + \boldsymbol{F}_{other}, \tag{2}$$

where $\boldsymbol{M}$ is the mass matrix and $\ddot{\boldsymbol{X}}$ is the acceleration. Equation (2) can be rewritten in a convolution integral form as follows:

$$\begin{aligned}(\boldsymbol{M} + \boldsymbol{A}_\infty)\ddot{\boldsymbol{X}} + \mathbf{c}\dot{\boldsymbol{X}} + \boldsymbol{K}\boldsymbol{X} + \int_0^t \mathbf{R}(t-\tau)\dot{\boldsymbol{X}}(\tau)d\tau \\ = \boldsymbol{F}_{excitation} + \boldsymbol{F}_{mooring} + \boldsymbol{F}_{PTO} + \boldsymbol{F}_{hydrostatic} + \boldsymbol{F}_{other},\end{aligned} \tag{3}$$

where $\boldsymbol{A}_\infty$ is the added mass at infinite frequency, $\mathbf{c}$ is the linear damping, $\boldsymbol{K}$ is the total stiffness and $\mathbf{R}$ is the retardation function. The hydrodynamic force is divided into two parts. On the left-hand side, the radiation force is represented by $\boldsymbol{A}_\infty\ddot{\boldsymbol{X}}$, which resembles an inertia force, and the convolution term $\int_0^t \mathbf{R}(t-\tau)\dot{\boldsymbol{X}}(\tau)d\tau$. The other part is the wave excitation force $\boldsymbol{F}_{excitation}$, which includes the force due to incident and diffracted waves. $\boldsymbol{F}_{other}$ represents any other forces, for example, the viscous drag force.

The solving process of the WEC dynamics problem is conducted by DNV SESAM SIMA V4.2-00, which enables coupled mooring dynamic analysis and instantaneous hydrostatic force calculation [34]. The fully coupled simulation procedure enables the simultaneous solution of the equation of motions for the WECs and the mooring lines.

3. Numerical Model

3.1. The Bottom-Fixed Heaving Point Absorber WEC

Figure 1 illustrates the WEC prototype and the numerical model of CorPower Ocean's WEC. There are two coordinate systems: lowercase letters represent the local coordinates,

while capital letters represent the global coordinates. The model consists of a wave buoy with a droplet shape, a stiff mooring line, a seabed anchor node and drag elements. The stiff mooring line provides negative axial stiffness, which amplifies the heave motion of the buoy with a value of −510 kN/m. This value was chosen based on the experiments and tuning of the WEC carried out by CorPower Ocean AB (Hägersten, Sweden). It is called a stiff mooring line because it has high bending stiffness so that the buoy moves only along the mooring line's axial direction. To avoid an extremely large force and violation of the assumption of linear potential theory, which requires small motions, the negative stiffness is set to 0 when the heave motion amplitude in the axial direction of the mooring line exceeds 2.5 m. As the weight of the WEC is far less than the weight of the water displaced by the WEC, the WEC is pre-tensioned by the stiff mooring line to balance extra buoyance. The seabed node is an anchor joint, which allows rotations around the x and y axes. The basic properties of the CorPower WEC system are listed in Table 1.

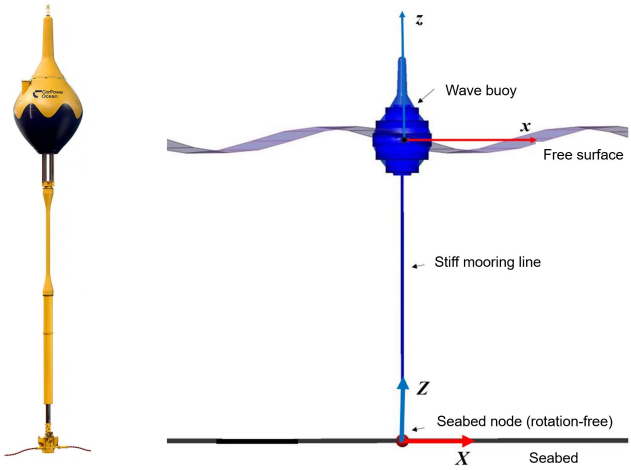

(**a**) (**b**)

Figure 1. (**a**) The WEC prototype and (**b**) the numerical model.

Table 1. Basic properties of the CorPower Ocean WEC system.

Property	Value
Mass [kg]	60.0×10^3
Draft [m]	5.421
Diameter [m]	9
Volume [m^3]	200
Centre of gravity, COG_w [m] [1]	−0.314
Roll inertia relative to COG_w, I_{xx} [kg × m^2]	2.5×10^6
Pitch inertia relative to COG_w, I_{yy} [kg × m^2]	2.5×10^6
Yaw inertia relative to COG_w, I_{zz} [kg × m^2]	5.0×10^5
Water depth [m]	46.0 or 55.0
Pre-tension [N]	1.4×10^6

[1] The origin of the reference Cartesian coordinate system (x, y, z) is placed on the plane of the water surface at the geometric centre of the WEC buoy when it is in its unloaded neutral position.

3.2. Drag Elements

The drag elements are designed to include the viscous drag force, which is not included in the linear potential flow theory. The viscous force is assumed to be of comparable magnitude with the inertial force since the WEC dimension is close to wave amplitude values. In Figure 2, the location of the drag elements is shown in local coordinates. There are six cylindrical drag elements in total to represent the varying dimensions of the buoy along the vertical direction. The radius and height of each drag element are listed in Table 2.

The drag coefficients of heave and surge/sway, 0.25 and 0.50, respectively, were provided by CorPower Ocean AB through their experience. The viscous forces in surge, sway and heave directions are calculated as follows:

$$F_{v,surge} = -\frac{1}{2} C_{D,surge} \rho A_{wet,z} |u_x| u_x, \tag{4}$$

$$F_{v,sway} = -\frac{1}{2} C_{D,sway} \rho A_{wet,z} |u_y| u_y, \tag{5}$$

$$F_{v,heave} = -\frac{1}{2} C_{D,heave} \rho A_3 |u_z| u_z, \tag{6}$$

where u_x, u_y and u_z are the surge, sway and heave velocities. A_3 is the cross-section area of the drag element D3. $A_{wet,z}$ represents the project area of the wetted element in the z-direction, as follows:

$$A_{wet,z} = \sum_{wet\ elements} 2R_i H_i \tag{7}$$

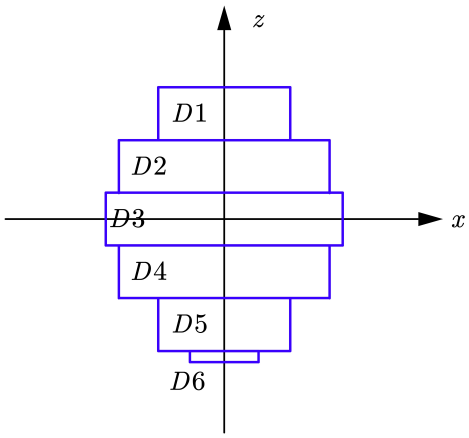

Figure 2. Arrangement of the drag elements in local coordinates.

Table 2. Parameters of the drag elements.

Drag Element No.	Radius R [m]	Height H [m]
D1	2.5	2.00
D2	4.0	2.00
D3	4.5	2.00
D4	4.0	2.00
D5	2.5	2.00
D6	1.3	0.42

3.3. PTO System

The PTO system of the WEC model is present inside the buoy. This PTO system is supposed to travel in an axial direction along the stiff mooring line. The PTO is simplified as a linear damper whose properties are introduced in Section 3.4. Moreover, when the device moves, it is necessary to ensure that the heave motions are restricted within the pre-defined limits to avoid damaging the device. This is taken care of by end-stop bumpers, which are modelled by introducing a non-linear force F_{es}. This force varies according to the following curve:

$$F_{es}(z) = -c \frac{z}{|z|} (|z| - z_{es})^n \cdot H(|z| - z_{es}) \tag{8}$$

where z_{es} is the end-stop distance beyond which the end-stop bumpers become active, and z is the vertical position in local coordinates. The constants c and n are altered to obtain the desired results. $H(\cdot)$ is the Heaviside step function. The nonlinear stiffness force curves

defined with different values of n are shown in Figure 3. The parameter n directly affects the degree of the equation: the larger the value of n, the higher the slope of the stiffness force. The value of n was set to 2 and the c value was set to 1×10^8 N/m^2. The z_{es} used in this WEC is 3.4 m.

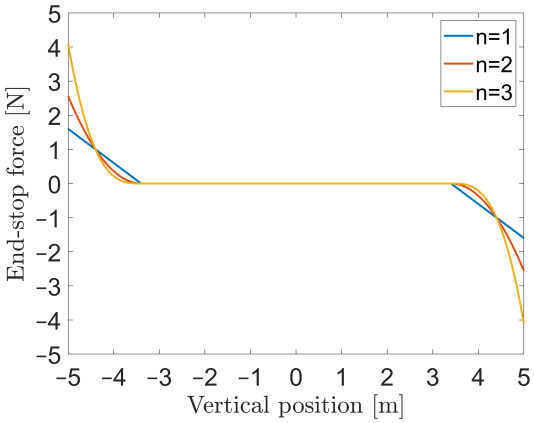

Figure 3. Non-linear stiffness force defined with different n values for the end-stop damper.

3.4. Power Performance Calculation

The wave energy harnessed from this WEC unit primarily comes from the heave motions of the buoy. The absorbed hydrodynamic power is calculated as follows:

$$P_{PTO} = C_{PTO}\dot{Z}_{rel}^2. \quad (9)$$

Here, C_{PTO} is the damping coefficient of the PTO, and $\dot{Z}_{rel}$ is the heave velocity of the buoy in global coordinates. The power output of the WEC unit varies depending on the characteristics of the wave to which it is subjected. Therefore, to determine its hydrodynamic performance characteristics, the power output is calculated for different wave characteristics, represented as sea states in Table 3. The damping coefficient is defined as follows:

$$C_{PTO} = R_u + R_{loss}. \quad (10)$$

The term R_{loss} is the linear damping loss, including machinery losses, and is set to a constant value of 25 kNs/m. This value was provided by CorPower Ocean AB based on their experimental data. The term R_u represents the useful damping consisting of various damping force elements, which change depending on the sea state the WEC is encountering. The useful damping also accounts for the damping from the generator. The values of R_u under different sea state conditions are presented in Table 3.

Table 3. Regular wave and irregular sea state conditions in the numerical simulations.

	Sea State	Wave Height [m]	Wave Period [s]	Useful Damping [kNs/m]	Direction
Regular Low	RL 1	1	5	137	0°
	RL 2	1	6	115	0°
	RL 3	1	7	94	0°
	RL 4	1	8	80	0°
	RL 5	1	9	78	0°
	RL 6	1	10	88	0°
	RL 7	1	11	107	0°
	RL 8	1	12	129	0°
	RL 9	1	13	152	0°
	RL 10	1	14	176	0°
	RL 11	1	15	199	0°

Table 3. *Cont.*

	Sea State	Wave Height [m]	Wave Period [s]	Useful Damping [kNs/m]	Direction
Regular High	RH 1	4	5	144	0°
	RH 2	4	6	124	0°
	RH 3	4	7	107	0°
	RH 4	4	8	163	0°
	RH 5	4	9	227	0°
	RH 6	4	10	287	0°
	RH 7	4	11	343	0°
	RH 8	4	12	395	0°
	RH 9	4	13	445	0°
	RH 10	4	14	494	0°
	RH 11	4	15	541	0°
Irregular Low	IRL 1	1.75	7.5	90	0° or 4.7°
	IRL 2	1.75	9.5	86	0° or 9.4°
	IRL 3	1.75	11.5	118	0° or 14°

The power output is evaluated in terms of the averaged useful power during the simulation time, which is calculated as follows:

$$P_u = \frac{1}{T}\int_0^T R_u \dot{Z}_{\text{rel}}^2 \, dt. \tag{11}$$

In Section 5, the power refers to P_u.

4. Study Cases

This section presents the cases studied in numerical simulations. In Section 4.1, two WEC array layouts are presented, which have been simulated and analysed for various WEC distances and sea state conditions. For all cases with regular wave conditions, the total simulation time was 1000 s; for irregular wave conditions, the total was 3 h.

4.1. Single WEC and Park Simulations

The two basic array layouts are shown in Figure 4. Each layout comprises 16 WECs arranged with a separation distance d between the WECs in the horizontal and vertical directions. The 4×4 layout has four WECs in each row and four in each column. The 8×2 layout consists of eight WECs in each of the two rows. This layout is wider and has more columns than the 4×4 layout. The intention behind these two layouts is to keep the same area but vary the number of rows and WECs in each row to analyse their interaction effects on the power generation capacity of WEC arrays. The regular square and rectangular shapes also reduce the potential challenges during the installation of multiple WECs and the deployment of electricity cables.

Table 3 presents the simulated sea state condition sets classified as regular waves (R) and irregular sea states (IR) where the JONSWAP spectrum with a peak enhancement factor of 2.4 was used. The regular waves are divided into sets of low (L) and high (H) waves for periods of 5 to 15 s, denoted by RL 1 to 11 and RH 1 to 11, whereas the three irregular sea states are denoted as IRL 1 to 3. These sea conditions cover the entire range of wave periods and wave heights that are of concern during the operation phase of WECs. The irregular sea states were defined by CorPower Ocean AB and reflect realistic sea state conditions at future installation sites.

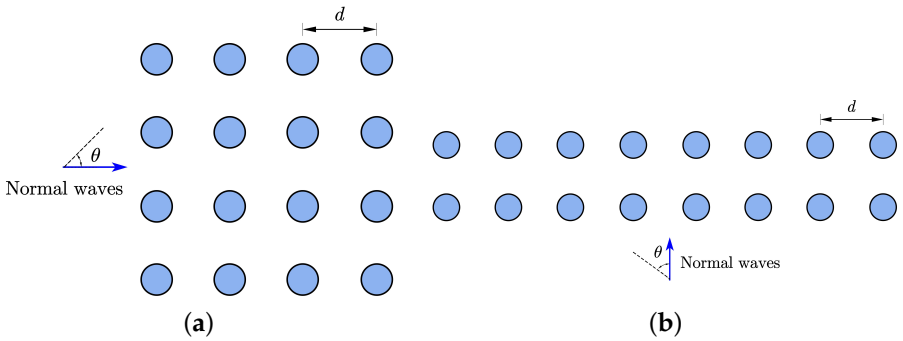

Figure 4. Basic array layouts used as study cases: (**a**) 4 × 4 and (**b**) 8 × 2.

5. Results and Discussion

5.1. Validation of the Single WEC Unit

Figure 5 presents the results from a numerical free decay test simulation. The simulation's purpose was to numerically obtain the WEC's resonance characteristics in heave and surge motions. The heave and surge resonant periods are observed as 8.5 and 17 s, respectively, and are aligned with the resonant periods of the real physical prototype of the WEC measured by CorPower Ocean AB. Therefore, the simulation model is validated in terms of its resonance characteristics.

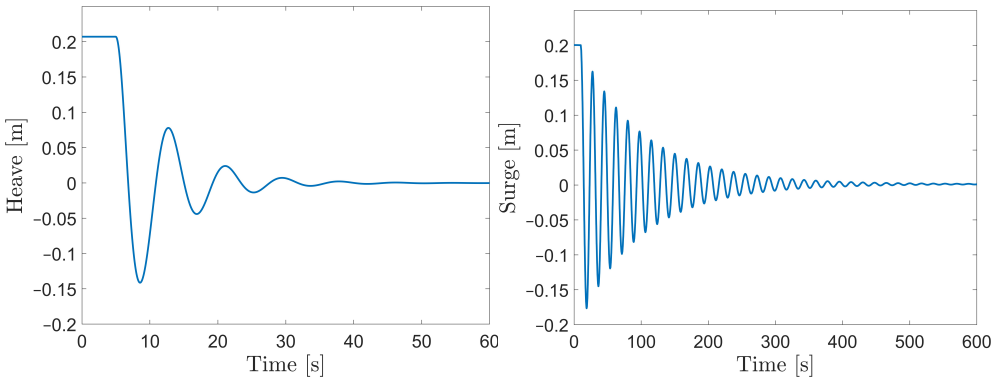

Figure 5. Motions of the WEC model in the free decay test simulations: (**a**) heave and (**b**) surge.

5.2. Effects of Wave Periods and Wave Heights on Power Performance

Figure 6a shows the total useful power output from simulations of the 4 × 4 array layout with a 150 m distance between the WECs. Results from several regular wave conditions are presented for the wave heights 1 m and 4 m. There is a drop in the power output when the wave periods are between 7 and 10 s. This is caused directly by the motion pattern of the WEC, shown in Figure 7. The upward motion range can be up to +4 m, whereas the downward motion can only reach −3 m. A hypothesis for this abnormal motion response observed for all WECs in the array is that it is caused by parametric resonance. The basis for this hypothesis is that parametric resonance is usually observed when the excitation frequency is twice the natural frequency of the system. This is exactly the case as the power drop happens for wave periods between 7 and 10 s, which are around half of the surge resonance period 17 s. The parametric resonance results in a large surge motion, which restricts the range of the translation motion of the WEC along the stiff mooring line. However, validating this hypothesis is beyond the scope of the current study and is left for future work. In addition, the maximum total power output of the array from the simulations is 10.9 MW with a wave height of 4 m and only 0.8 MW with a 1 m wave height. Note that the wave height is increased four times from 1 to 4 m, while the power output is increased more than ten times. This demonstrates the considerable influence of wave height on the power output.

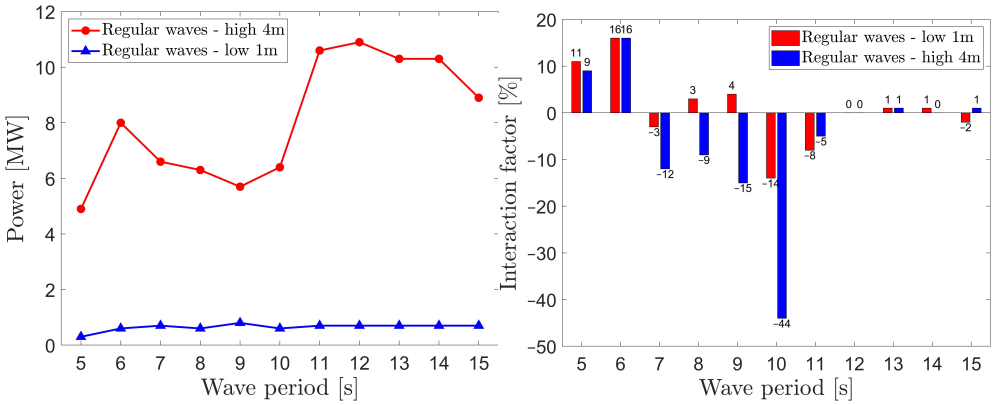

(**a**) (**b**)

Figure 6. (**a**) Power output of the 4 × 4 array layout (d = 150 m) for the regular wave conditions RL 1 to 11 and RH 1 to 11; see Table 3 for details. (**b**) Interaction factors for the cases presented in (**a**); see the text for details.

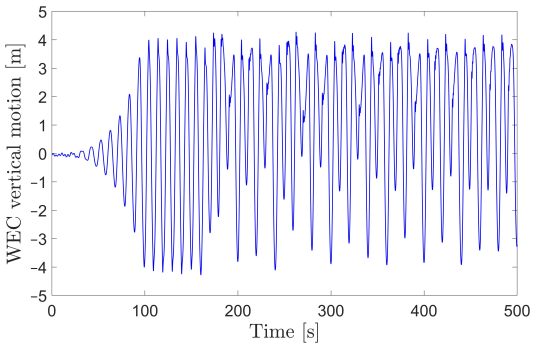

Figure 7. Illustration of an abnormal heave motion response of a WEC near resonance. Under regular waves, the wave height is 4 m, and the wave period is 10 s.

An interaction factor was defined as the percentage of the power difference between an array and the same number of single units under the same sea state condition and with other parameters the same to evaluate the influence of interaction effects. The interaction factor of the 4 × 4 array layout is shown in Figure 6b. At the short wave periods of 5 s and 6 s, the power output is enhanced by interaction effects by at least 9% and up to 16%. For longer wave periods, from 12 to 15 s, the influence of interaction on the power performance is less than 1%. This indicates that waves with short wave periods are preferable for enhancing power performance, while waves with long periods have a negligible influence on power performance.

5.3. Effects of Water Depth on Power Performance

At the real installation site, the water depth may vary due to the seabed's changing topography, which changes the wave load on the WECs. The rod length that connects the buoy to the seabed should also be changed accordingly. These changes may affect the power performance. Therefore, two cases with 46 m and 55 m were simulated to study the influence of water depth on the power performance. Figure 8 shows the influence of water depth on the power output for the 4 × 4 array layout with a distance of 150 m. The simulations were carried out for the IRL 1 to IRL 3 sea states presented in Table 3. The results show a 1% increase in power performance for the deeper water depth. The reason for this minor positive effect is that a longer mooring line is needed for the 55 m water depth, which enables a larger range of global surge motion and, consequently, a larger range of translation along the stiff mooring line. Overall, the changing water depth has a negligible influence on the interaction effects since the interaction factors are similar for different water depths.

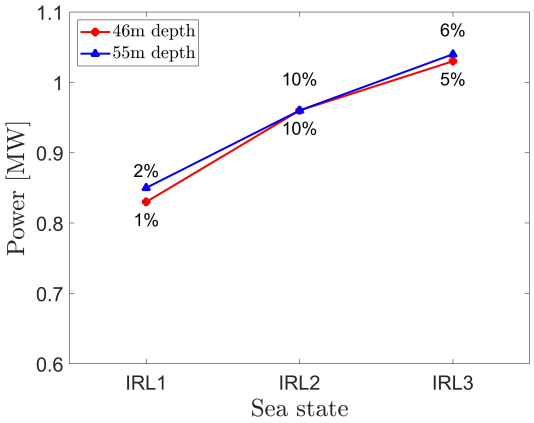

Figure 8. Power output of the 4 × 4 array layout (d = 150 m) for the water depths 46 m and 55 m and the irregular sea states IRL 1 to 3. The percentages are the interaction factors indicating the additional power generation due to interaction effects.

5.4. Effects of the Array layout on Power Performance

The influence of the array layout on the power output is presented in Figure 9. The simulations were carried out for the IRL 1 to 3 sea states presented in Table 3. The interaction factor is calculated for each IRL sea state and indicated by the percentage values.

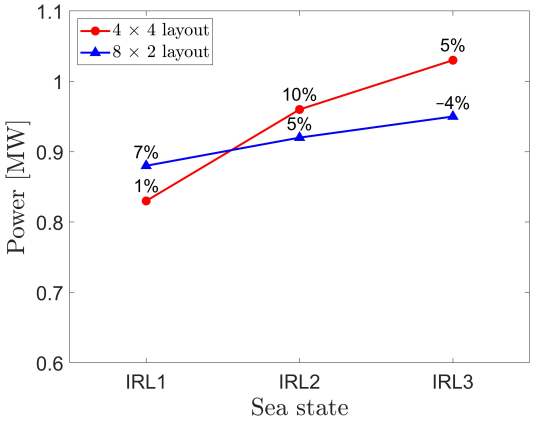

Figure 9. Power output of the 4 × 4 and 8 × 2 array layouts (d = 150 m) for the irregular sea states IRL 1 to 3. The percentages are the interaction factors indicating the additional power generation or power reduction due to interaction effects.

The 8 × 2 array layout performs better than the 4 × 4 array layout for IRL 1. This result can be explained by the results presented in Figure 10. For the 8 × 2 array layout with a 0-degree incident wave direction, all eight units in the first (upstream) row experience lower negative interaction effects than the 4 × 4 array layout. However, the second (downstream) row produces less power, probably due to the shielding effects of the first row. There is a significant power output drop for the 8 × 2 array in columns C5 and C6. The possible reason for this phenomenon is that their neighbours, C4 and C7, show large power increases due to positive interaction effects. For the 4 × 4 array layout, the downstream rows after the first-row experience higher negative interaction effects that reduce the motion and power output of the WECs.

Under IRL 2 and 3, the interaction effects are more favourable for the 4 × 4 array layout, while the 8 × 2 array layout experiences destructive interactions at IRL 3 and produces 4% less than the case without interaction. This is caused by the fact that the performance of the WECs in the second and third rows of the 4 × 4 array layout is enhanced by interaction effects while the performance of the first row of the 8 × 2 array layout is greatly reduced, as shown in Figure 11.

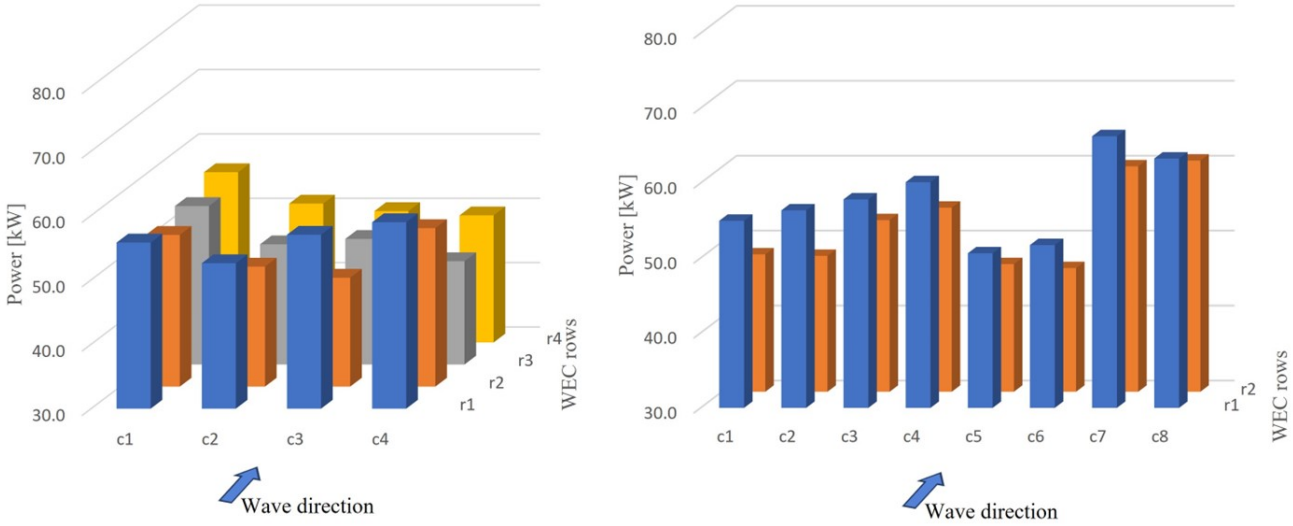

Figure 10. Power output of individual WEC units in the 4 × 4 (**left**) and 8 × 2 (**right**) array layouts (d = 150 m) for the IRL 1 sea state.

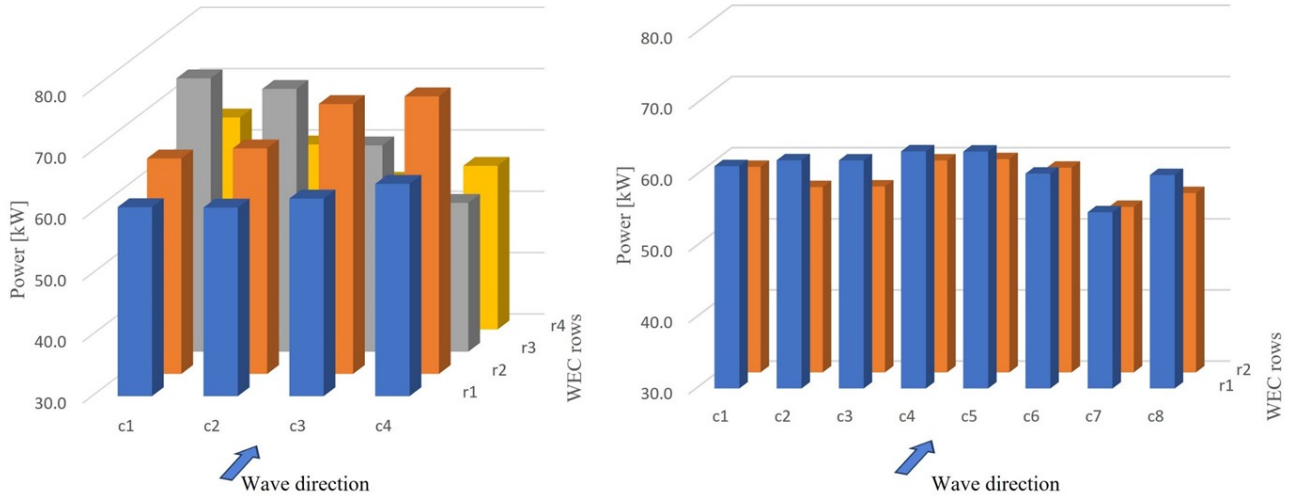

Figure 11. Power output of individual WEC units in the 4 × 4 (**left**) and 8 × 2 (**right**) array layouts (d = 150 m) for the IRL 3 sea state.

5.5. Effects of Wave Directions on Power Performance

The influence of the wave direction on the power output for the 4 × 4 array layout is presented in Figure 12. The red line represents the power at the 0-degree wave direction for the IRL 1 to 3 sea states (d = 150 m); the dark blue line represents the same sea states with the wave directions 4.7 degrees, 9.4 degrees and 14.0 degrees, respectively. The trend for the 0-degree case is upward, as is observed in the previous cases for the increased wave period. The percentages represent the increased positive power output due to interaction effects. The interaction is more significant in IRL 2 for the 9.4-degree wave direction as it produces 5% more power than the case without interaction at the 0-degree wave direction for IRL 2. However, normal waves are preferable for IRL 2 and IRL 3 as they enable higher power boosts of 10% and 5%, respectively, compared to their counterparts with incoming wave angles.

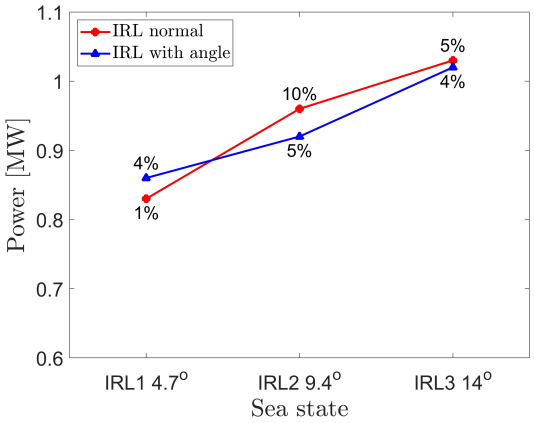

Figure 12. Power output of the 4 × 4 array layout (d = 150 m) for different wave directions and the irregular sea states IRL 1 to 3. The percentages are the interaction factors indicating the additional power generation due to interaction effects.

5.6. Effects of WEC Distances on Power Performance

Figure 13a shows the power output of the 4 × 4 array layout with different distances between the WECs for the RL 1 to 11 simulation cases. The case without interaction does not consider the radiation and diffraction effects from the WEC units in the numerical model. Its power output equals 16 isolated WECs under the corresponding sea state. It is included for comparison purposes in array layout simulations. When the wave period increases from 5 to 7 s, i.e., from RL 1 to 3, the power output is positively related to the wave period. However, from RL 4 to 9, the power output of all distances decreases due to the previously mentioned parametric resonance. Figure 13b shows the interaction factors that share the exact definition as shown in Figure 6b. It can be seen that the 150 m WEC distance is favourable since it enables a relatively large power output increase under RL 1 and 2 and avoids a possible large power output reduction under RL 3 to 11.

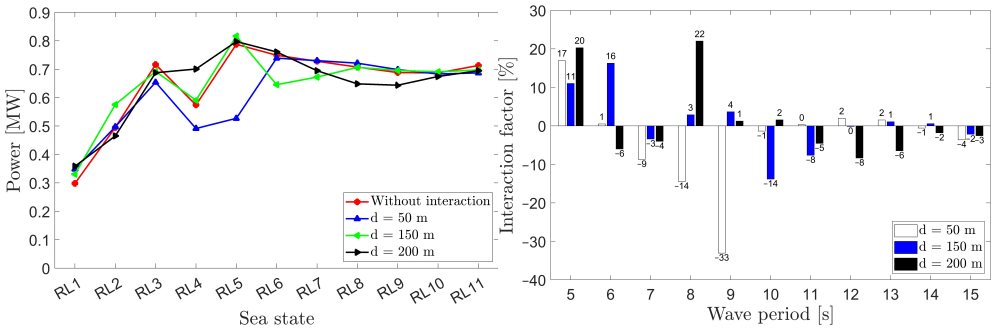

(**a**) (**b**)

Figure 13. (**a**) Power output of the 4 × 4 array layout for different WEC distances for regular wave conditions RL 1 to 11. (**b**) Interaction factors for different WEC distances under regular wave conditions RL 1 to 11.

6. Conclusions

A numerical model is put forward to extend the margin of the computational capacity of BEM for wave park simulations. By developing new strategies for the numerical setup, this BEM-based model can model 16 instances at once, while also considering a detailed PTO system. Like the previous development in the family of BEM methods, the present BEM-based model considers all hydrodynamic and structural-dynamic interaction effects.

The bottom-fixed heaving point absorber WEC designed by CorPower Ocean was used to simulate and analyse interaction effects in relation to the array layout wave parks. Several factors varied, such as regular wave and irregular sea state conditions, water depth, wave encounter direction, and WEC distance in the array.

The influence of wave height on the hydrodynamic performance was found to be large. One example of simulation results showed that increased wave height in regular wave conditions with a factor of four increased the power output ten times. Water depth was studied for two cases, 46 m and 55 m, and there was a marginal difference in power output. The latter showed an increase in power output by 1% compared to the former.

The simulation results showed a clear influence of the interaction effects between WECs. They verify what previous researchers have found in experiments and numerical simulations. Each WEC type and array design must be studied carefully for many sea state conditions to find an appropriate distance between the WECs and array layout, to generate power outputs where the interaction factor is beneficial compared to single WEC installations. In this study, for example, the 8×2 array layout performed better for IRL 1, while the 4×4 array layout performed better for IRL 2 and 3. Regarding the distance between WECs, a 150 m distance seems to be the most favourable if all simulation results are included in the overall assessment since it results in the highest power production in total.

Author Contributions: Conceptualization, X.S., J.W.R., H.-D.Y. and J.H.T.; methodology, X.S., J.W.R. and H.-D.Y.; software, X.S., U.R.S.L.G. and H.N.K.; Writing—original draft, X.S., U.R.S.L.G. and H.N.K.; Writing—review & editing, J.W.R., H.-D.Y. and J.H.T.; Project administration, J.W.R.; Funding acquisition, J.W.R. All authors have read and agreed to the published version of the manuscript.

Funding: This work was performed within the projects 'Control of wave energy converters based on wave measurements, for optimal energy absorption', funded by the Swedish Energy Agency through contract agreement no. 50197-1, and 'INTERACT—Analysis of array systems of wave energy converters with regard to interaction effects in the LCoE and fatigue analyses', funded by the Swedish Energy Agency through contract agreement no. 50148-1. This work also received funding from the Chalmers University of Technology Foundation for the strategic research project 'Hydro- and aerodynamics'.

Institutional Review Board Statement: Not applicable.

Informed Consent Statement: Not applicable.

Data Availability Statement: The data that support the findings of this study are available within the article.

Conflicts of Interest: Author Jørgen Hals Todalshaug was emplo yed by the company CorPower Ocean AB. The remaining authors declare that the research was conducted in the absence of any commercial or financial relationships that could be construed as a potential conflict of interest.

References

1. Thorpe, T.W. *A Brief Review of Wave Energy*; A Report Produced for the UK Department of Energy, No ETSU R120; The UK Department of Trade and Industry: London, UK, 1999.
2. Clément, A.; McCullen, P.; Falcão, A.; Fiorentino, A.; Gardner, F.; Hammarlund, K.; Lemonis, G.; Lewis, T.; Nielsen, K.; Petroncini, S.; et al. Wave energy in Europe: Current status and perspectives. *Renew. Sustain. Energy Rev.* **2002**, *6*, 405–431. [CrossRef]
3. Falnes, J. A review of wave-energy extraction. *Mar. Struct.* **2007**, *20*, 185–201. [CrossRef]
4. Falcao, A.F.d.O. Wave energy utilization: A review of the technologies. *Renew. Sustain. Energy Rev.* **2010**, *14*, 899–918. [CrossRef]
5. Budal, K. Theory for absorption of wave power by a system of interacting bodies. *J. Ship Res.* **1977**, *21*, 248–254. [CrossRef]
6. Falnes, J. Radiation impedance matrix and optimum power absorption for interacting oscillators in surface waves. *Appl. Ocean Res.* **1980**, *2*, 75–80. [CrossRef]
7. Yang, S.H.; Ringsberg, J.W.; Johnson, E. Wave energy converters in array configurations—Influence of interaction effects on the power performance and fatigue of mooring lines. *Ocean Eng.* **2020**, *211*, 107294. [CrossRef]
8. Li, X.; Xiao, Q.; Zhou, Y.; Ning, D.; Incecik, A.; Nicoll, R.; McDonald, A.; Campbell, D. Coupled CFD-MBD numerical modeling of a mechanically coupled WEC array. *Ocean Eng.* **2022**, *256*, 111541. [CrossRef]
9. Krivtsov, V.; Linfoot, B. Basin Testing of Wave Energy Converters in Trondheim: Investigation of Mooring Loads and Implications for Wider Research. *J. Mar. Sci. Eng.* **2014**, *2*, 326–335. [CrossRef]
10. Babarit, A. Impact of long separating distances on the energy production of two interacting wave energy converters. *Ocean Eng.* **2010**, *37*, 718–729. [CrossRef]
11. Stallard, T.; Stansby, P.K.; Williamson, A.J. An experimental study of closely spaced point absorber arrays. In Proceedings of the ISOPE International Ocean and Polar Engineering Conference, Vancouver, BC, Canada, 6–11 July 2008; p. ISOPE-I.

12. Göteman, M. Wave energy parks with point-absorbers of different dimensions. *J. Fluids Struct.* **2017**, *74*, 142–157. [CrossRef]
13. Vasiliki, L.; Areti, L.; Eva, L. Hydrodynamic Interaction Effects and Performance of an Offshore Wave Farm. In Proceedings of the Twenty-Seventh 2017 International Ocean and Polar Engineering Conference, San Francisco, CA, USA, 25–30 June 2017; pp. 207–214.
14. Weller, S.; Stallard, T.; Stansby, P. Experimental measurements of irregular wave interaction factors in closely spaced arrays. *IET Renew. Power Gener.* **2010**, *4*, 628–637. [CrossRef]
15. Lee, H.; Poguluri, S.; Bae, Y. Performance Analysis of Multiple Wave Energy Converters Placed on a Floating Platform in the Frequency Domain. *Energies* **2018**, *11*, 406. [CrossRef]
16. Hu, J.; Zhou, B.; Vogel, C.; Liu, P.; Willden, R.; Sun, K.; Zang, J.; Geng, J.; Jin, P.; Cui, L.; et al. Optimal design and performance analysis of a hybrid system combing a floating wind platform and wave energy converters. *Appl. Energy* **2020**, *269*, 114998. [CrossRef]
17. Ghafari, H.R.; Ghassemi, H.; Abbasi, A.; Vakilabadi, K.A.; Yazdi, H.; He, G. Novel concept of hybrid wavestar- floating offshore wind turbine system with rectilinear arrays of WECs. *Ocean Eng.* **2022**, *262*, 112253. [CrossRef]
18. Jin, P.; Zheng, Z.; Zhou, Z.; Zhou, B.; Wang, L.; Yang, Y.; Liu, Y. Optimization and evaluation of a semi-submersible wind turbine and oscillating body wave energy converters hybrid system. *Energy* **2023**, *282*, 128889. [CrossRef]
19. Zhou, B.; Hu, J.; Jin, P.; Sun, K.; Li, Y.; Ning, D. Power performance and motion response of a floating wind platform and multiple heaving wave energy converters hybrid system. *Energy* **2023**, *265*, 126314. [CrossRef]
20. Zhu, K.; Shi, H.; Zheng, S.; Michele, S.; Cao, F. Hydrodynamic analysis of hybrid system with wind turbine and wave energy converter. *Appl. Energy* **2023**, *350*, 121745. [CrossRef]
21. Göteman, M.; Engström, J.; Eriksson, M.; Isberg, J. Optimizing wave energy parks with over 1000 interacting point-absorbers using an approximate analytical method. *Int. J. Mar. Energy* **2015**, *10*, 113–126. [CrossRef]
22. Göteman, M.; Engström, J.; Eriksson, M.; Isberg, J. Fast Modeling of Large Wave Energy Farms Using Interaction Distance Cut-Off. *Energies* **2015**, *8*, 13741–13757. [CrossRef]
23. Stratigaki, V.; Troch, P.; Stallard, T.; Forehand, D.; Kofoed, J.P.; Folley, M.; Benoit, M.; Babarit, A.; Kirkegaard, J. Wave basin experiments with large wave energy converter arrays to study interactions between the converters and effects on other users in the sea and the coastal area. *Energies* **2014**, *7*, 701–734. [CrossRef]
24. Rahm, M.; Svensson, O.; Boström, C.; Waters, R.; Leijon, M. Experimental results from the operation of aggregated wave energy converters. *IET Renew. Power Gener.* **2012**, *6*, 149–160. [CrossRef]
25. da Fonseca, F.C.; Gomes, R.; Henriques, J.; Gato, L.; Falcão, A. Model testing of an oscillating water column spar-buoy wave energy converter isolated and in array: Motions and mooring forces. *Energy* **2016**, *112*, 1207–1218. [CrossRef]
26. Wolgamot, H.A.; Taylor, P.H.; Taylor, R.E.; Van Den Bremer, T.; Raby, A.; Whittaker, C. Experimental observation of a near-motion-trapped mode: Free motion in heave with negligible radiation. *J. Fluid Mech.* **2016**, *786*, R5. [CrossRef]
27. Mercadé Ruiz, P.; Ferri, F.; Kofoed, J.P. Experimental validation of a wave energy converter array hydrodynamics tool. *Sustainability* **2017**, *9*, 115. [CrossRef]
28. Sinha, A.; Karmakar, D.; Soares, C.G. Performance of optimally tuned arrays of heaving point absorbers. *Renew. Energy* **2016**, *92*, 517–531. [CrossRef]
29. Tay, Z.Y.; Venugopal, V. Hydrodynamic interactions of oscillating wave surge converters in an array under random sea state. *Ocean Eng.* **2017**, *145*, 382–394. [CrossRef]
30. Shao, X.; Ringsberg, J.W.; Yao, H.D.; Li, Z.; Johnson, E.; Fredriksson, G. A comparison of two wave energy converters' power performance and mooring fatigue characteristics—One WEC vs many WECs in a wave park with interaction effects. *J. Ocean Eng. Sci.* **2023**, *8*, 446–460. [CrossRef]
31. Newman, J.N. *Marine Hydrodynamics*; The MIT Press: Cambridge, MA, USA, 2018.
32. Faltinsen, O. *Sea Loads on Ships and Offshore Structures*; Cambridge University Press: Cambridge, UK, 1993; Volume 1.
33. HydroD. 2024. Available online: https://www.dnv.com/services/hydrodynamic-analysis-and-stability-analysis-software-hydrod-14492 (accessed on 7 April 2024).
34. SIMA. SIMA Documenattion. 2024. Available online: https://sima.sintef.no/doc/4.4.0/sima/index.html (accessed on 7 April 2024).